Albumin–Folate Conjugates for Drug-targeting in Photodynamic Therapy

Kathrin Butzbach[1], Federico A.O. Rasse-Suriani[2], M. Micaela Gonzalez[2], Franco M. Cabrerizo[2]* and Bernd Epe[1]*

[1]Institute of Pharmacy and Biochemistry, University of Mainz, Mainz, Germany
[2]Instituto de Investigaciones Biotecnológicas - Instituto Tecnológico de Chascomús (IIB-INTECH), Universidad Nacional de San Martín (UNSAM) - Consejo Nacional de Investigaciones Científicas y Técnicas (CONICET), Chascomús, Argentina

ABSTRACT

Photodynamic therapy (PDT) is based on the cytotoxicity of photosensitizers in the presence of light. Increased selectivity and effectivity of the treatment is expected if a specific uptake of the photosensitizers into the target cells, often tumor cells, can be achieved. An attractive transporter for that purpose is the folic acid receptor α (FRα), which is overexpressed on the surface of many tumor cells and mediates an endocytotic uptake. Here, we describe the synthesis and photobiological characterization of polar β-carboline derivatives as photosensitizers covalently linked to folate-tagged albumin as the carrier system. The particles were taken up by KB (human carcinoma) cells within <90 min and then colocalized with a lysosomal marker. FRα antibodies prevented the uptake and also the corresponding conjugate without folate was not taken up. Accordingly, a folate-albumin-β-carbolinium conjugate proved to be phototoxic, while the corresponding albumin–β-carbolinium conjugates without FA were nontoxic, both with and without irradiation. An excess of free folate as competitor for the FRα-mediated uptake completely inhibited the photocytotoxicity. Interestingly, the albumin conjugates are devoid of photodynamic activity under cell-free conditions, as shown for DNA as a target. Thus, phototoxicity requires cellular uptake and lysosomal degradation of the conjugates. In conclusion, albumin–folate conjugates appear to be promising vehicles for a tumor cell targeted PDT.

INTRODUCTION

In photodynamic therapy (PDT), the cytotoxicity of singlet oxygen and free radicals generated from intracellular photosensitizers is exploited to selectively kill cells in irradiated tissues (1,2). At present, PDT is successfully applied for the treatment of various types of cancer (*e.g.* skin, bladder and esophagus), actinic keratosis and macular degeneration (3–7). Drugs suitable for PDT have to fulfil a number of photophysical prerequisites such as high absorption coefficients at long wavelengths and high triplet quantum yields. Moreover, they have to be nontoxic in the dark and exhibit favorable pharmacokinetic characteristics with respect to the distribution in the body, metabolism and excretion.

The systemic use of photosensitizers can cause side effects in noncancerous tissues such as a severe sensitization of the skin and eyes to light. Therefore, an important goal for the improvement of PDT is the combination of photosensitizers with delivery systems that allow an accumulation of the drugs in the target cells (mostly tumor cells) prior to the irradiation with light (8–10). This would constitute a second selectivity filter in addition to that one obtained by local irradiation. For cytostatic drugs, various types of delivery systems have already been established and some have been approved for medication in humans (11). Thus, antibodies recognizing tumor-specific antigens on the surface of cells can serve as vehicles for an endocytotic uptake of small toxic drugs that have been covalently linked to the antibody, a principle that is now successfully applied in breast cancer therapy (12). Another group of delivery systems make use of the fact that many tumor cells overexpress the high-affinity folate receptor FRα (K_D <1 nM), which acts by receptor-mediated endocytosis (13–15). FRα specifically recognize folic acid (FA) even when covalently bound to a macromolecule or nanoparticle. The FA, together with the attached payload, is delivered to endosomes or lysosomes. (16) A FRα-mediated uptake was shown for direct (low-molecular weight) conjugates between FA and photosensitizers (17,18) and has been demonstrated for photosensitizers and other drugs covalently or noncovalently attached to many different kinds of macromolecular vehicles such as liposomes, nanotubes, graphene or proteins (reviewed in (19)).

The targeting of proteins and nanoparticles to tumor tissue is further increased by the enhanced permeability and retention (EPR) effect (20). It results from the fact that blood vessels in tumor tissues are strongly fenestrated and often lack a smooth muscle layer. Moreover, the lymphatic drainage is reduced at these sites. Hence, molecules bigger than 40 kDa often accumulate in tumor tissue, but not in healthy tissue. Albumin has been recognized as a favorable drug-targeting vehicle because it is well tolerated and exhibits a strong EPR effect, which may be partly mediated by the glycoprotein gp60 (21,22). Thus, an albumin-conjugated taxane derivative was approved for use in metastatic breast cancer (23).

To test whether the FRα-mediated uptake can be exploited for a tumor-targeted PDT, we covalently coupled a photosensitizer to bovine serum albumin (BSA) and subsequently linked the conjugate to FA. Here, we show that covalent conjugates of albumin with polar β-carboline derivatives as photosensitizers and attached FA residues as targeting moieties are subject to a FRα-mediated uptake into tumor cells. In consequence, the

*Corresponding authors' emails: fcabrerizo@intech.gov.ar (Franco M. Cabrerizo); epe@uni-mainz.de (Bernd Epe)

albumin-β-carbolinium-FA particles proved to be cytotoxic in the presence of light, while albumin-β-carbolinium conjugates without FA were nontoxic, both with and without irradiation.

MATERIALS AND METHODS

Cells, antibodies and other materials. KB cells (assumed to be HeLa cell derivatives) were obtained from the Leibniz-Institute DSMZ, Braunschweig, Germany (ACC 136). HaCaT cells, which are immortalized human keratinocytes, were obtained from N.E. Fusenig (DKFZ, Heidelberg, Germany). Cells were cultured in high-glucose Dulbecco's modified Eagle's medium (Gibco, Darmstadt, Germany) containing the normal concentration of FA (9 μM), supplemented with 10% fetal calf serum (FCS), 1% penicillin/streptomycin, and 1% glutamine. FA (>99%), superoxide dismutase (SOD), catalase, N-hydroxy-succinimide (NHS), 1-ethyl-3-(3-dimethylaminopropyl)carbodiimid (EDC) and N-cyclohexyl-N'-(2-morpholinoethyl)carbodiimide methyl-p-toluenesulfonate (CMC) were obtained from Sigma–Aldrich. Albumin fraction V ≥ 98% (BSA) was from Carl Roth GmbH und Co KG (Karlsruhe, Germany). WST-1 reagent was purchased from Roche Applied Science (Mannheim, Germany). DNA from bacteriophage PM2 was prepared according to the method of Salditt *et al.* (24). Formamidopyrimidine-DNA glycosylase (Fpg) was partially purified from inducible overproducing *Escherichia coli* strains (JM105 carrying the plasmid pFPG239) (25). The mounting medium ProLong© Gold antifade reagent, LysoTracker© Red, MitoTracker© Deep Red and NucRed© 647 nm were obtained from life technologies (Darmstadt, Germany).

Synthesis of 2-(2-carboxyethyl)-β-carbolinium cations (cnHo and cHa). To a stirred air-equilibrated solution of β-carboline (100 mg, 0.6 mmol) and 3-iodopropionic acid (1200 mg, 6 mmol) in methanol (50 mL), a solution of sodium hydroxide (240 mg, 6 mmol) in methanol (50 mL) was added dropwise to neutralize the former solution. The reaction was stirred in the absence of light at room temperature until TLC indicated that the reaction was complete. The reaction mixture was then evaporated in a rotary evaporator to give a pale yellow solid residue. Products were isolated by flash column chromatography (200–400 mesh 60 Å and ethyl acetate–methanol mixtures as eluent) to give as white solids. ^{1}H- and ^{13}C-NMR spectra were recorded in dimethylsulfoxide-d_6 at 500 MHz (see Supporting Information). All the solvents used were analytical grade and were freshly distilled and dried before using. Norharmane (nHo) and harmine (Ha), sodium hydroxide and 3-iodopropionic acid were purchased from Sigma-Aldrich.

Synthesis of albumin-β-carbolinium and albumin-β-carbolinium–folate conjugates. Albumin (10 mg mL^{-1} equivalent to 150 μM) was stirred with 1.5 mM of the β-carboline in the presence of 5 mM EDC and 5 mM NHS at room temperature for 24 h in water. The reaction mixture was dialysed (>30 kDa) against PBS, repeatedly concentrated and resuspended in water by means of Centriprep© centrifugation (NMWL >30 kDa) and lyophilized. Half of the product subsequently was redissolved in water and coupled to folate following the protocol of Fischer *et al.* (26). After purification as described for the albumin-β-carbolinium, the product was stored after lyophilization. Purity was checked by photometric and fluorimetric monitoring of the Centriprep© filtrate.

UV-MALDI-TOF MS. Samples were measured on a Shimadzu Axima CFR MALDI-TOF MS with a pulsed nitrogen laser (λ = 337 nm, 3 ns). The used matrix was sinapinic acid. 5 μL of sample solution (c = 1 g L^{-1}) was mixed with 25 μL of matrix solution (c = 10 g L^{-1}). The solvent was acetonitrile/0.1% trifluoroacetic acid in a ratio of 1:1.

Analysis of damage induced in cell-free PM2 DNA. PM2 DNA (10 000 bp) was irradiated at a concentration of 10 μg mL^{-1} in the presence of different concentrations of β-carbolines or its albumin conjugates in phosphate buffer (5 mM KH$_2$PO$_4$, 50 mM NaCl, pH 7.4) on ice in 96-well plates for 20 min with a Philips HPW 125-W mercury lamp emitting at 365 nm, placed at a distance of 10 cm, equivalent to 30 kJ m^{-2}. The subsequent quantification of DNA modifications induced in cell-free DNA was carried out by means of a relaxation assay (27,28). In brief, an aliquot of 0.2 μg DNA in 20 μL BE$_1$ buffer (20 mM Tris–HCl, pH 7.5, 100 mM NaCl, 1 mM EDTA) was incubated for 30 min at 37°C with 10 μL of BE$_1$ buffer (for the determination of directly produced single-strand breaks [SSB]) or 10 μL of Fpg protein

(3 μg mL^{-1}) in BE$_1$ buffer. Under the incubation conditions, the latter enzyme converts all substrate DNA modifications into SSB. The reactions were terminated by addition of 10 μL of 1% sodium dodecyl sulphate and the DNA was applied to an agarose electrophoresis gel. Fluorescence scanning of the relaxed and supercoiled forms of the DNA after staining with ethidium bromide allowed us to calculate the number of SSBs or — if an incubation with a repair enzyme Fpg protein preceded the gel electrophoresis — the number of SSBs plus Fpg-sensitive modifications. The number of Fpg-sensitive sites was obtained by subtraction of the number of SSBs.

To test for the involvement of superoxide anion radicals ($O_2^{\bullet-}$) and hydrogen peroxide (H_2O_2) in the DNA damage generation, the PM2 DNA together with different β-carboline concentrations was irradiated with either catalase (315 U mL^{-1}) or SOD (200 μg mL^{-1}) or both. To test for the participation of singlet oxygen, the irradiation was done in buffer-containing D_2O instead of H_2O and the pD was adjusted according to Srere *et al.* (29).

Analysis of cell viability. KB cells were plated in 96-well plates (7000 per well). After 24 h, they were incubated for 90 min with different amounts of β-carboline or the corresponding BSA-conjugates. Afterwards cells were washed with PBS and irradiated from the top of the cell culture dish without plastic cover for 20 min with a Philips HPW 125-W mercury lamp emitting at 365 nm, placed at a distance of 10 cm, equivalent to 30 kJ m^{-2}. After irradiation and washing with PBS (and, in some cases, an incubation under culture conditions for 24 h), 100 μL of culture medium with 10 μL WST-1 reagent was added to every well. The tetrazolium dye in the WST-1 reagent gets reduced to a formazan by mitochondrial enzymes and color changes from red to yellow in the presence of vital cells. The increase of the absorption at 450 nm measured directly after addition of the reagent and exactly 2 h later is an indicator of the metabolic activity and therefore viability of the cells. The relative viability was calculated as the ratio of the increase in absorption in treated cells and control cells (not exposed to β-carbolinium derivatives).

Fluorescence microscopy. KB cells were plated on cover slips (18 mm, Nr. 1.5) in 12-well-plates (100 000 per well). After 24 h, cells were incubated for various times with 20 μM albumin-β-carboline conjugates in PBS or – in some experiments with extended incubation times (≥90 min) – in a culture medium. Afterwards cells were washed with PBS and fixed with ice-cold paraformaldehyde (PFA, 4%). Thirty minutes prior to fixation, LysoTracker© Red (50 nM) or MitoTracker© DeepRed (100 nM) or two drops of NucRed© 647 nm were added to each well for staining. The cover slips were put on mounting medium on object slides and analyzed with a TCS SP5 confocal fluorescence microscope, using excitations at 405 nm for β-carboline, 560 nm for LysoTracker© Red, and 633 nm for MitoTracker© DeepRed and NucRed© 647 nm. Images were taken and processed with Leica Application Suite X software and Image J©.

Statistical analysis. An analysis of variance (ANOVA) was carried out to calculate the statistical significance of the results (P values). Significance levels are indicated by asterisks (* for $P < 0.05$; *** for $P < 0.005$).

RESULTS

Synthesis and photophysical characterization of free β-carbolinium cations and their conjugates

Two novel β-carbolinium derivatives, namely 2-(2-carboxyethyl)-norharmanium (cnHo) and 2-(2-carboxyethyl)-harminium (cHa) cations were selected as photosensitizers to study the FRα-mediated uptake and the resulting phototoxicity in KB carcinoma cells, which previously have been shown to strongly express FRα under our culture conditions (30). The absorption spectra and main photophysical parameters of the two compounds are shown in Figure S1a and Table 1 respectively.

cnHo shows a higher fluorescence quantum yield (Φ_F) and longer fluorescence lifetime (τ_F) than cHa. Moreover, the lowest energy absorption band of cnHo shows a bathochromic shift (~50 nm) with respect to cHa (Figure S1a). This makes cnHo

Table 1. Main photophysical parameters determined upon one-photon excitation of 2-(2-carboxyethyl)-β-carbolinium cations in pH 7.4 air-equilibrated aqueous solution.

	λ_{max}^{Abs} [nm]	λ_{max}^{Flu} [nm]	φ_F*	τ_F [ns]†	φ_Δ‡
cnHo	374	485	0.58 ± 0.02	21.9 ± 0.1	0.05 ± 0.02
cHa	326	425	0.42 ± 0.02	6.8 ± 0.1	0.14 ± 0.02

*Fluorescence quantum yield. †Fluorescence lifetime. ‡Singlet oxygen quantum yield (φ_Δ), determined in air-equilibrated D_2O solutions.

suitable for the microscopic analysis of the cellular uptake and the subcellular distribution. On the other hand, cHa has a higher quantum yield of excited triplet states and, in consequence, singlet oxygen production (Φ_Δ) than cnHo, allowing an efficient photochemical reactivity (photosensitized damage generation). Therefore, in the following studies cnHo was used as a chromophore for fluorescence-based experiments, while cHa was chosen for cytotoxicity studies. As quaternary ammonium ions, both compounds are highly polar, which minimizes diffusion-mediated cellular uptake of the free photosensitizers.

Both β-carbolinium derivatives were covalently linked to albumin by carbodiimide coupling to yield cnHo-Alb and cHa-Alb respectively. Analysis by UV-MALDI-TOF MS revealed that under the experimental conditions used each albumin molecule bound one or two cnHo and cHa residues. The albumin conjugates were subsequently coupled with an excess of FA to yield cnHo-Alb-FA and cHa-Alb-FA respectively. Thereby, about 7–10 folate residues were attached to the β-carbolinium–albumin conjugates according to photometric measurements and UV-MALDI-TOF MS analysis (Fig. 1). An analysis by protein gel electrophoresis (Figure S2) confirms the covalent nature of the labeling.

Extent and mechanism of damage generation by β-carbolinium cations and their conjugates

To judge and compare the potency of the β-carbolinium derivatives as photosensitizers and to analyze the mechanism(s) underlying their photoreactivity, we carried out experiments with cell-free DNA as a target. The numbers of SSB and DNA modifications sensitive to Fpg protein generated by the compounds under irradiation in the presence of supercoiled PM2 DNA was quantified by means of a relaxation assay, as described previously (27,28). Fpg protein is a repair glycosylase that recognizes both oxidized purines such as 8-oxoG and sites of base loss (AP sites) (31). The results shown in Fig. 2 indicate that both cnHo and cHa give rise to a concentration-dependent formation of both SSB and Fpg-sensitive modifications in the DNA, while no DNA damage is generated by the β-carbolines without irradiation or by the irradiation alone (data not shown). The Fpg-sensitive sites prevail over SSB by a factor of 7.3 for cnHo and 2.1 for cHa. Such a preponderance of base modifications is characteristic for many photosensitizers damaging via Type-I and Type-II reaction (see below) (32). The cHa is approx. 30-fold more potent as damaging agent than cnHo in the case of the Fpg-sensitive sites and 100-fold in the case of the SSB, as calculated from the linear slopes of the concentration-dependent data in Fig. 2. Note that the latter comparison is allowed because the two β-carbolinium derivatives have quite similar total absorption of the incident

light used in the above-mentioned experiments (see Figure S1b and c). The much higher photodynamic activity of cHa in comparison to cnHo is in accordance with previous results for the parental β-carbolines (not substituted at the pyridinic nitrogen of the main β-carboline ring) (33). The higher potency of cHa is not fully explained by its higher singlet oxygen quantum yield (Table 1), but might indicate a more favorable redox potential of the photoexcited cHa. Very similar ratios were observed previously also with respect to the relative induction of the two types of DNA modification that were quantified (33). The absolute extent of DNA damage is increased by the quaternization of the nitrogen atom by a factor of 2 in the case of cnHo and a factor of 12 in the case of cHa.

Mechanistically, photosensitized damage can be generated in a direct reaction of the excited state of the photosensitizer with the substrate, most often by one-electron abstraction (the so-called Type-I reaction) or indirectly via reactive oxygen species (ROS) (the so-called Type-II reaction) (34). In the latter case, an energy or electron transfer reaction with molecular oxygen generates singlet oxygen ($^1O_2$) or superoxide anions ($O_2^{\bullet-}$) respectively, which then give rise to damage formation in secondary reactions. In order to test for ROS as intermediates in the DNA damage generation by cHa, the irradiations were carried out in the presence of catalase, SOD or in D_2O as solvent. The results (Fig. 3) exclude a significant involvement of hydrogen peroxide, superoxide and singlet oxygen in the generation of SSB. The observed two-fold increase of the yield of Fpg-sensitive modifications in D_2O as solvent indicates that singlet oxygen (at least partially) contributes to the generation of this type of lesion, which is consistent with the fact that singlet oxygen selectively generates guanine modifications and only few SSB (32).

When the albumin conjugate of cHa (cHa-Alb) was analyzed for DNA damage generation under the same conditions as the free cHa, virtually no damage was detected (Fig. 2). This indicates that either the albumin-bound photosensitizer has no access to the target DNA to allow a direct reaction or the excited chromophore immediately reacts with the albumin as the preferential substrate. In support of this conclusion, the photoreactivity with DNA can be partly restored by incubation of the conjugate with proteinase K (data not shown).

FRα-mediated uptake of albumin conjugates into KB cells

After the photodynamic activity of the β-carbolinium compounds was established, we studied the time-dependent uptake of the albumin conjugates into KB cells by confocal fluorescence microscopy. The experiments were carried with the conjugates of cnHo, namely cnHo-Alb-FA and cnHo-Alb because of the superior fluorescence yield of this chromophore. The results (Fig. 4a) indicate that cnHo-Alb-FA, but not cnHo-Alb (lacking the folate residues) is increasingly taken up within an incubation period of 90 min. As shown in Fig. 4b, the β-carboline fluorescence co-localizes in the cells at least partly with that of LysoTracker©. No co-localization is observed with MitoTracker© DeepRed and with NucRed© 647 nm, indicating that the photosensitizer does not significantly accumulate in the mitochondria or in the nucleus of the target cells (Figures S3 and S4 respectively). The presence of free FA (1 mM) in the medium during the incubation with cnHo-Alb-FA strongly inhibits the cellular uptake of cnHo (Fig. 4c). This is an indication that the uptake of the cnHo-Alb-
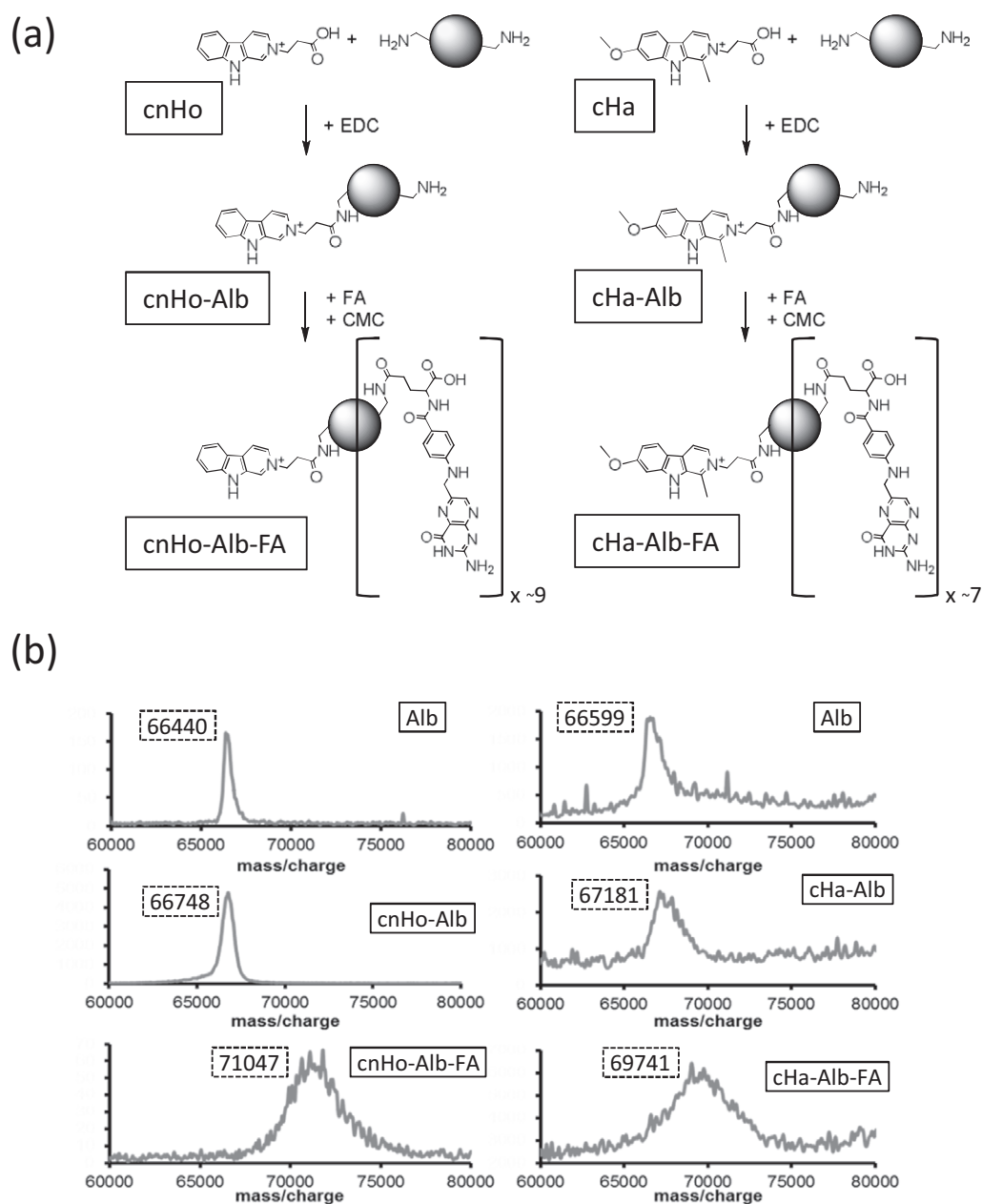
Figure 1. (a) Structures and synthesis of the albumin conjugates used in this study. (b) UV-MALDI-TOF mass spectra of the albumin conjugates and albumin.

FA conjugate is indeed receptor mediated. The transport by FRα is further confirmed by the observation that the uptake of cnHo-Alb-FA is also prevented by pre-incubation of the KB cells with an anti-FRα-IgG (Figure S5).

The uptake of cnHo-Alb-FA and cnHo-Alb was also compared for longer incubation periods (≥90 min) in culture medium. The results (shown in Figure S4) show no significantly better uptake of cnHo-Alb-FA after 6 h compared to that after 90 min. After 24 h, but not after 6 h, the pictures indicate some – apparently FR-α-independent – uptake of cnHo-Alb. The data suggest that very long incubation times might reduce the selectivity for FR-α-positive cells.

As a control cell line previously demonstrated to express only few or no FRα (30), we used immortalized human keratinocytes (HaCaT cells). No significant uptake of cnHo-Alb-FA was observed in these cells (Figure S6), in support of the assumption that the observed uptake by KB cells is mediated by FRα.

Phototoxicity of β-carbolinium conjugates in KB cells

The phototoxicities of free cHa and its two conjugates (cHa-Alb and cHa-Alb-FA) were analyzed by a viability assay measuring the metabolic activity via intracellular formazan formation from a tetrazolium salt (WST-1). The results (Fig. 5) indicate the absence of phototoxicity for cHa and cHa-Alb, even after long pre-incubation time up the highest concentrations applied (20 μM). In contrast, the conjugate endowed with folate residues (cHa-Alb-FA) proved moderately, but significantly, phototoxicity already at 5 μM. The phototoxicity did not increase further at concentrations >10 μM and did not exceed a level of 20% dead
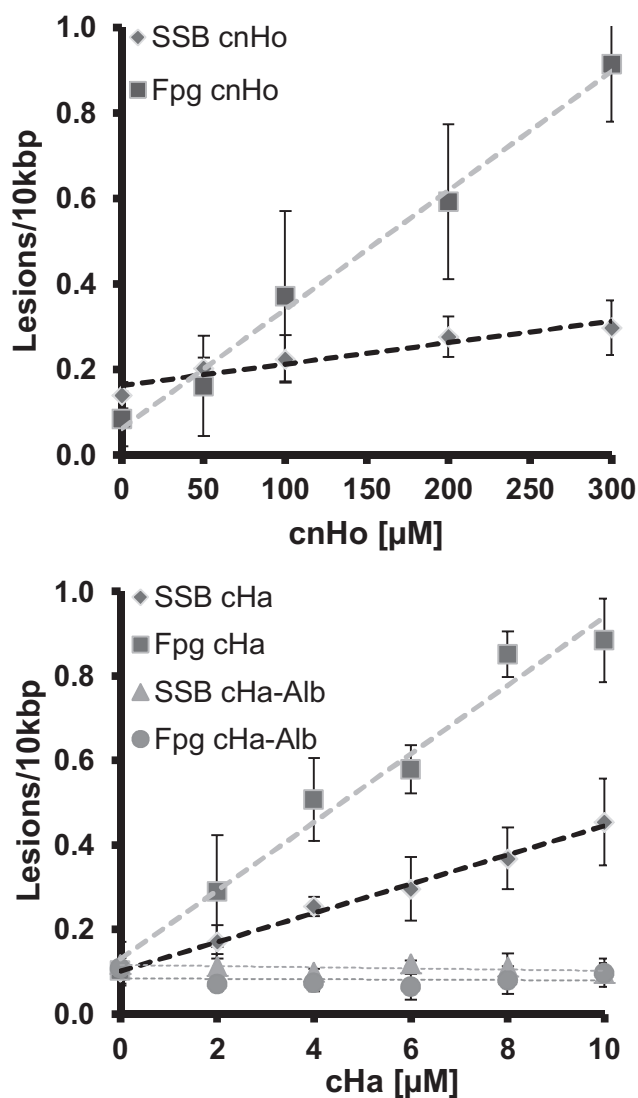
Figure 3. Influences of catalase, SOD and D_2O on the generation of SSBs and Fpg-sensitive modifications in DNA by cHa under irradiation with UVA (365 nm; 30 kJ m^{-2}). The concentrations of cHa were 20 μM for SSB and 5, 10 and 20 μM for Fpg-sensitive lesions respectively. The number of modifications observed in phosphate buffer with cHa alone was normalized to 100%. Numbers of lesions significantly different from those in the control incubations (100%) are indicated by asterisks. Data are means of 3 (for SSB) or 6 (for Fpg-sensitive sites) independent experiments ±SD.

Figure 2. Numbers of DNA modifications generated by photoexcited cnHo (upper panel), cHa and cHa-Alb (lower panel) under cell free conditions. PM2 DNA in phosphate buffer was exposed to increasing concentrations of the compound plus UVA (365 nm; 30 kJ m^{-2}). The numbers of SSB and of modifications sensitive to Fpg were determined in a relaxation assay. Data are means of three independent experiments (±SD).

cells, possibly because the receptor-mediated uptake of the conjugate is saturated under these conditions. For all the compounds, no cytotoxicity was observed in the dark (Figure S7). The irradiation alone was not associated with any cytotoxicity (data not shown).

To test whether cytotoxicity develops only slowly after irradiation, *e.g.* due to a delayed induction of apoptosis, the metabolic activity was also quantified 24 h after irradiation. The cytotoxicities measured with the WST-1 assay after that time were very similar to those obtained directly after irradiation (Figure S8). Most probably, all cells prone to die are already detected as metabolically inactive by the WST assay shortly after irradiation, *i.e.* the succinate dehydrogenase inhibition (determined in the WST assay) is mostly likely an early event in the induction of cell death.

To verify the relevance of FRα in the phototoxicity of cHa-Alb-FA, the pre-incubation was carried out in the presence of a
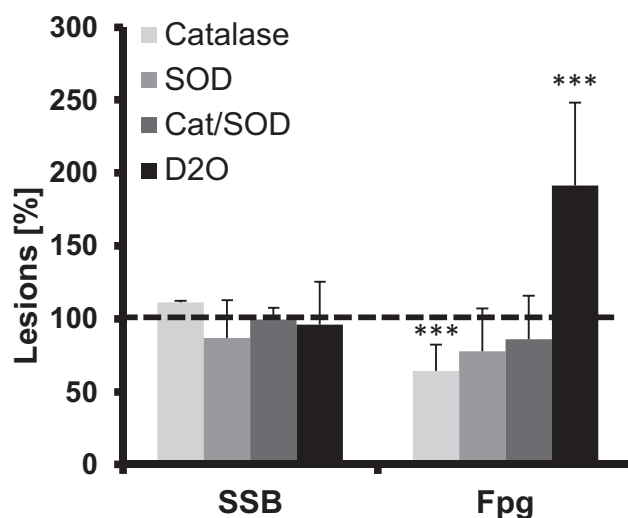
high excess of free FA as competitor for the receptor. The subsequent irradiation was carried out in the absence of cHa-Alb-FA and free FA, as in the other cases. The results (Fig. 6) indicate a complete inhibition of the phototoxicity induced by cHa-Alb-FA. The influence of FA calculated by multiple regression analysis is highly significant ($P = 0.004$). It has to be concluded that the observed phototoxicity is completely dependent on a receptor-mediated uptake of the photosensitizer–albumin conjugates.

As an additional control, we determined the phototoxicity of cHa and its albumin conjugates in HaCaT cells, lacking FRα (see above). In these cells, the compounds were devoid of measurable phototoxic effects (Figure S9).

DISCUSSION

The results show – to the best of our knowledge for the first time – that photosensitizers covalently linked to folate-tagged albumin can be used for a selective killing of cells expressing the folate receptor FRα. In this delivery system, three selectivity filters are combined for a preferential killing of malignant target cells in a tumorous tissue. Firstly, as characteristic for PDT, only irradiated cells are affected, provided that the photosensitizer is nontoxic in the dark. Secondly, albumin as a carrier efficiently accumulates in tumor tissues because of its very good EPR effect. Thirdly, folate receptors of the type FRα are often strongly expressed in tumor cells, but not in nonproliferating cells, in particular normally not on the basolateral membrane surface of epithelial blood vessel cells.

It is difficult to quantitatively transfer the (only weak) phototoxicity observed in this study to *in vivo* situations of PDT since the extent of cell killing depends directly on the intensity of the light source, its emission wavelength and the irradiation times. From the viewpoint of PDT, the β-carbolinium derivatives used in this study should (only) be regarded as model compounds for
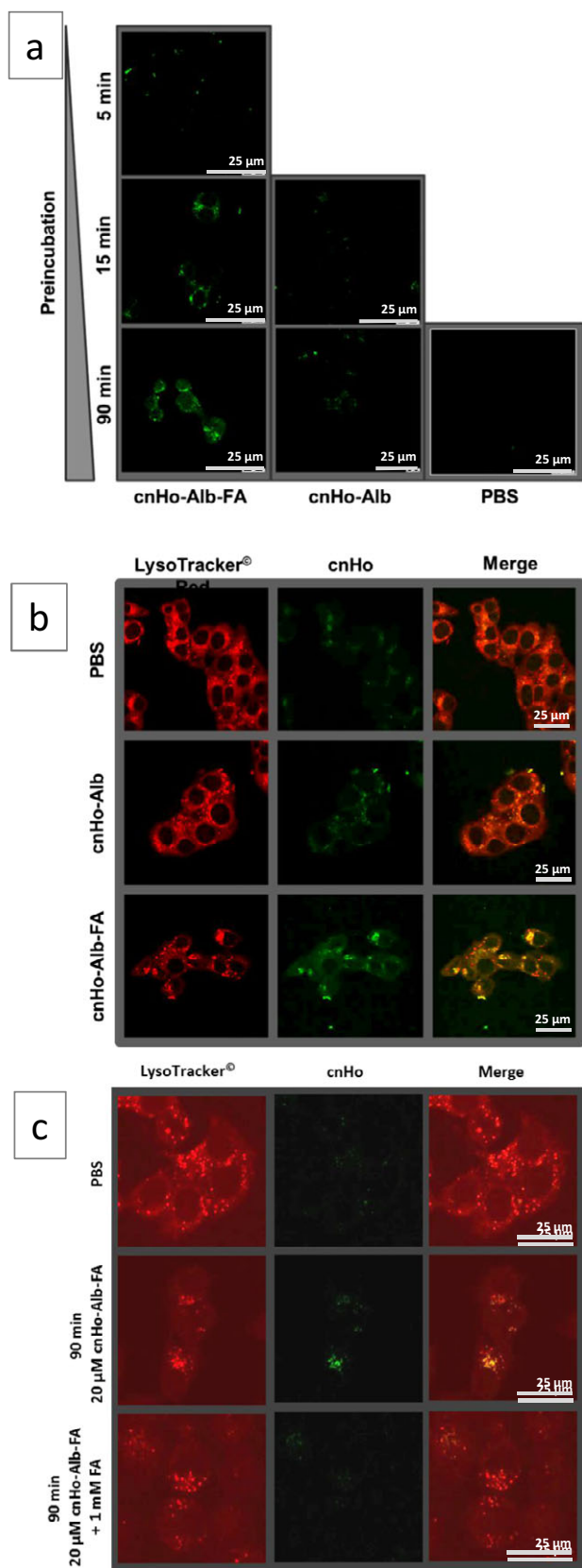
Figure 4. Fluorescence microscopy of KB cells after incubation with cnHo-Alb or cnHo-Alb-FA and, if indicated, LysoTracker© Red. The fluorescence of cnHo and LysoTracker© Red was visualized by excitation with a laser at 405 nm and 560 nm respectively. (a) The cells were incubated for the indicated times with cnHo-Alb or cnHo-Alb-FA, washed, and fixed with cold PFA (4%). (b) Cells were incubated for 90 min with cnHo-Alb or cnHo-Alb-FA and subsequently for 30 min with Lyso-Tracker© Red (50 nм). After washing, cells were fixed with cold PFA (4%). (c) Cells were incubated for 90 min with cnHo-Alb or cnHo-Alb-FA in the presence or absence of FA (1 mм) and subsequently for 30 min in LysoTracker© Red (50 nм). After washing, cells were fixed with cold PFA (4%).
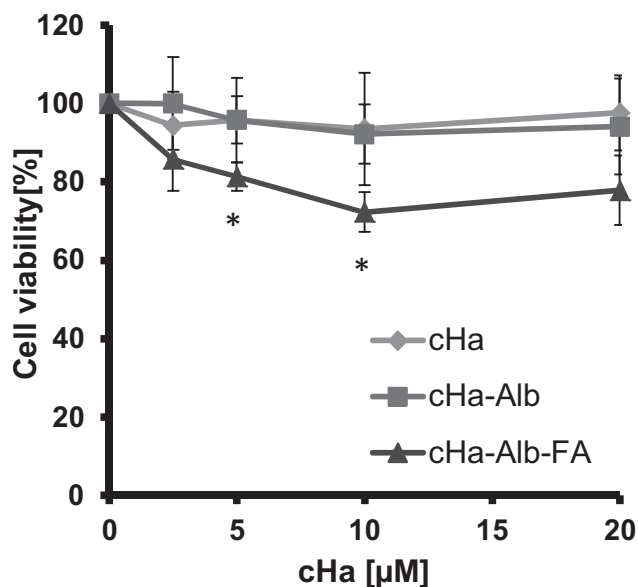

Figure 5. Viability of KB cells after incubation with cHa, cHa-Alb or cHa-Alb-FA for 90 min and subsequent irradiation for 20 min with UVA (365 nm; 30 kJ m^{-2}) in PBS alone. The amount of formazan produced in a subsequent incubation (2 h) with WST-1 reagent was determined photometrically. The relative cell viability was calculated from the ratio of formazan produced in the treated cells and control cells that were irradiated in the absence of any photosensitizer. Data are means of 3 (for 5 and 10 µм) or 6 (for 0 and 20 µm) independent experiments ±SD. Significant differences ($P < 0.05$) at a given concentration between cHa-Alb-FA-treated and cHa-Alb-treated cells are indicated by an asterisk.

regular PDT, photosensitizers with absorption at longer wavelengths are required to obtain photodynamic effects in deeper layers of a target tissue. On the other hand, high hydrophilicity is required to avoid noncovalent interactions with albumin, which in the case of porphyrins have been shown to be difficult to reverse (data not shown). Suitable chromophores with high triplet yields and strong absorption at wavelengths >650 nm such as aza-BODIPY dyes are available (1,35) and could be derivatized in future studies in the way described (carboxyl moiety for carbodiimide coupling and cationic character to increase hydrophilicity). Interestingly, the β-carbolines used in this study could be useful in two-photon photodynamic therapy (TP-PDT) (36,37) since they have non-negligible two photon cross section values (at ~ 600–750 nm) (38,39).

It is interesting to note that covalent binding of the β-carbolinium cations to albumin completely inhibits their photodynamic activity, at least for DNA as a target (Fig. 3). Quenching effects of excited (triplet or singlet) states by albumin have previously been observed, *e.g.* for hematoporphyrin conjugates (40) and for
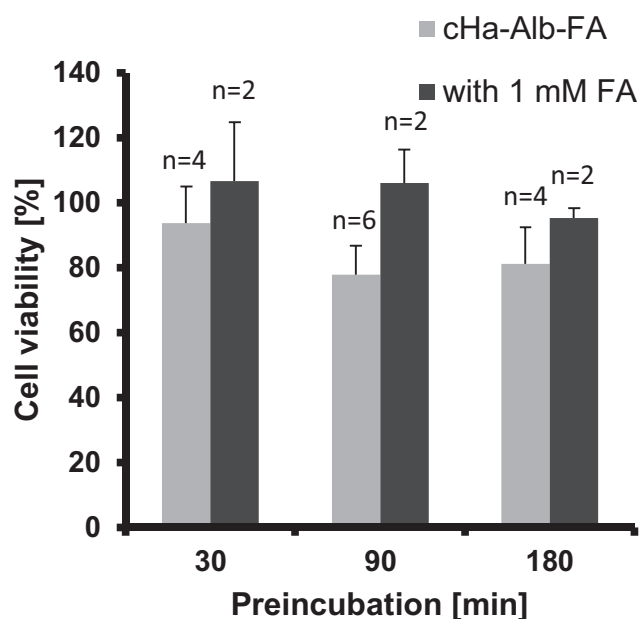
highly hydrophilic photosensitizers with suitable photophysical parameters and a free carboxyl moiety suitable for coupling to albumin by the carbodiimide technique. For an application in

Figure 6. Viability of KB cells after incubation for the indicated times with 20 μM cHa-Alb-FA in the absence and presence of FA (1 mM). After incubation, cells were irradiated for 20 min with UVA (365 nm; 30 kJ m^{-2}) in PBS alone. The amount of formazan produced in a subsequent incubation (2 h) with WST-1 reagent was determined photometrically. The relative cell viability was calculated from the ratio of formazan produced in the treated cells and control cells that were irradiated in the absence of any photosensitizer. Columns indicate means (±SD) from the indicated numbers of independent experiments. The significance of the FA influence calculated by ANOVA is $P = 0.04$.

zinc phthalocyanine, a type-II photosensitizer which noncovalently associates with the protein (41). From a therapeutic viewpoint, the internal quenching is advantageous, since it is expected to enhance the selectivity of the conjugates under PDT conditions because phototoxicity only results after cellular uptake and (lysosomal) degradation of the protein. Recently, this principle has been successfully applied in a mouse model of peritoneal carcinomas, using a conjugate of an anti-EGFP monoclonal antibody with the benzoporphyrin derivative (BPD) as the tumor-targeting photosensitizer (42). The observed co-localization of cnHo with a lysosomal marker after cellular uptake (Fig. 2b) is in accordance with the assumption that the photodynamic effect follows lysosomal degradation of the conjugate, as would be characteristic for a clathrin-dependent endocytosis, although a CLIC-GEEC-mediated uptake would be more characteristic for glycosyl phosphatidyl-anchored receptors such as FRα (16). There are indications, however, that multivalent folate conjugates (particles with several folates attached) indeed traffic mostly to lysosomes (19,43). A model proposed for the FAα-mediated uptake and subsequent phototoxicity of cHa-Alb-FA is shown in Fig. 7.

Covalent binding of photosensitizers to unsubstituted albumin (without folate residues) has already been shown to improve the accumulation of the photosensitizer in the tumor tissue of tumor-bearing mice (44), most probably as a result of the EPR effect of albumin. Similarly, improved tumor-specific biodistribution and photodynamic activities *in vivo* were also observed when glutaraldehyde-crosslinked albumin nanoparticles were noncovalently loaded with various photosensitizers (45,46). In these cases, a re-distribution of the photosensitizers to the target cells is expected to take place. Recently, hollow copper sulfide nanoparticles were coated with an albumin–folate conjugate and noncovalently loaded with a photosensitizer. The composites were shown to be more cytotoxicity under irradiation than in the dark and to allow receptor-mediated uptake (47).

Folate attached to albumin or albumin aggregates (nanoparticles) has been tested as targeting "warhead" for various types of cytostatic drugs. Thus, doxorubicin attached via an acid-labile linker to albumin, which was subsequently conjugated with folate residues, was shown to accumulate in FRα-expressing cells and improve the cytostatic effects *in vivo* (48). The linking of a paclitaxel–albumin conjugate with folate improved selectivity for FRα-positive cells (49). Receptor-mediated uptake and toxicity was also shown for glutaraldehyde-cross-linked albumin nanospheres noncovalently loaded with doxorubicin (50).

The damaging mechanism underlying the observed phototoxicity in the KB cells remains to be established. Free photosensitizer molecules present in the lysosomes after degradation of the attached albumin might give rise to a break-down of lysosomal membranes during irradiation and thus trigger lysosomal cell death (51,52). Damage to DNA may also play a role, although the cytotoxic potential of the DNA modifications predominantly induced by the β-carbolines (Fpg-sensitive base modifications and single-strand breaks, see Fig. 2) is relatively weak and the photosensitizers do not appear to accumulate in the nuclei of the cells (Figure S4). As concluded from the cell-free experiments
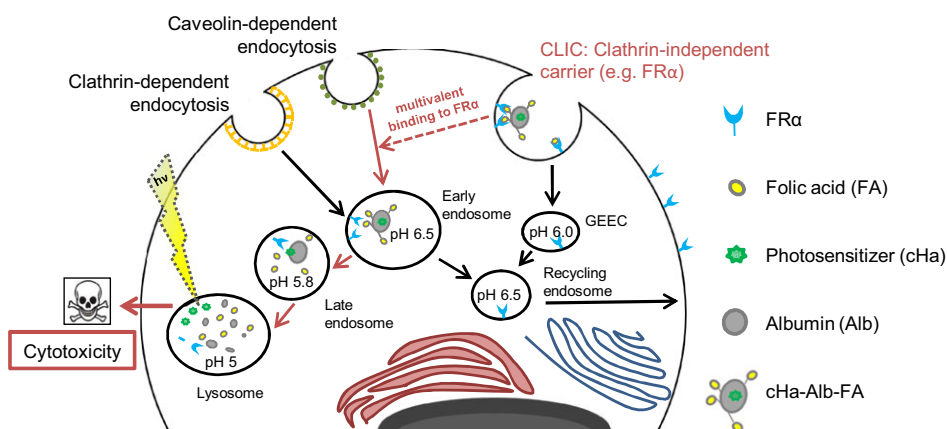

Figure 7. Proposed model for the FRα-mediated uptake and cytotoxicity of cHa-Alb.

(Fig. 3), ROS such as singlet oxygen or hydroxyl radicals do not appear to play a dominant role as ultimately damaging species, in agreement with previous findings for other β-carboline derivatives (33,53). Rather, direct (Type I) reactions seem to be responsible for the damage generation.

In conclusion, the covalent attachment of photosensitizers to folate-modified albumin appears to be a new strategy for PDT that completely avoids photocytotoxicity to cells lacking active endocytotic folate transport. The photophysical characteristics and the efficacy of the photosensitizer moiety probably can be optimized, and the distribution of the conjugates in tumor and nontumor tissues *in vivo* needs to be studied.

SUPPORTING INFORMATION

Additional Supporting Information may be found in the online version of this article:

Figure S1. (a) UV-vis absorption spectra and absorbed spectral photon fluxes of cnHo and cHa.

Figure S2. SDS PAGE of various albumin conjugates used in this study and of albumin visualized with UV-A excitation (upper panel) and Coomassie Blue staining (lower panel).

Figure S3. Fluorescence microscopy after incubation of KB cells with cnHo-Alb and cnHo-Alb-FA: co-localization with MitoTracker© DeepRed.

Figure S4. Fluorescence microscopy after incubation of KB cells with cnHo-Alb and cnHo-Alb-FA: co-localization with NucRed© 647 nm.

Figure S5. Influence of the presence of FRa antibodies on the uptake of cnHo-Alb-FA by KB cells.

Figure S6. Lack of uptake of cnHo-Alb and cnHo-Alb-FA by HaCaT cells.

Figure S7. Viability of KB cells after incubation with cHa, cHa-Alb and cHa-Alb-FA for 90 min in the dark.

Figure S8. Delayed cell viability of KB cells after pre-incubation with cHa, cHa-Alb or cHa-Alb-FA for 90 min and subsequent irradiation for 20 min with UVA (365 nm; 30 kJ m^{-2}) in PBS.

Figure S9. Cell viability of HaCaT cells after 90 min pre-incubation with 20 μM cHa or cHa-Alb and subsequent irradiation for 20 min with UVA (365 nm; 30 kJ m^{-2}) in PBS alone. NMR data. 1H- and 13C-NMR data of cnHo and cHa.

REFERENCES

1. O'Connor, A. E., W. M. Gallagher and A. T. Byrne (2009) Porphyrin and nonporphyrin photosensitizers in oncology: Preclinical and clinical advances in photodynamic therapy. *Photochem. Photobiol.* **85**, 1053–1074.
2. Juzeniene, A., Q. Peng and J. Moan (2007) Milestones in the development of photodynamic therapy and fluorescence diagnosis. *Photochem. Photobiol. Sci.* **6**, 1234–1245.
3. Brown, S. B., E. A. Brown and I. Walker (2004) The present and future role of photodynamic therapy in cancer treatment. *Lancet Oncol.* **5**, 497–508.
4. Agostinis, P., K. Berg, K. A. Cengel, T. H. Foster, A. W. Girotti, S. O. Gollnick, S. M. Hahn, M. R. Hamblin, A. Juzeniene, D. Kessel, M. Korbelik, J. Moan, P. Mroz, D. Nowis, J. Piette, B. C. Wilson and J. Golab (2011) Photodynamic therapy of cancer: An update. *CA Cancer J. Clin.* **61**, 250–281.
5. Babilas, P., S. Schreml, M. Landthaler and R. M. Szeimies (2010) Photodynamic therapy in dermatology: State-of-the-art. *Photodermatol. Photoimmunol. Photomed.* **26**, 118–132.
6. Simone, C. B. II and K. A. Cengel (2014) Photodynamic therapy for lung cancer and malignant pleural mesothelioma. *Semin. Oncol.* **41**, 820–830.
7. Wormald, R., J. Evans, L. Smeeth and K. Henshaw (2007) Photodynamic therapy for neovascular age-related macular degeneration. *Cochrane Database Syst. Rev.*, CD002030; DOI: 10.1002/14651858. CD002030.pub3
8. Sharman, W. M., J. E. van Lier and C. M. Allen (2004) Targeted photodynamic therapy via receptor mediated delivery systems. *Adv. Drug Deliv. Rev.* **56**, 53–76.
9. Bugaj, A. M. (2011) Targeted photodynamic therapy–a promising strategy of tumor treatment. *Photochem. Photobiol. Sci.* **10**, 1097–1109.
10. Shirasu, N., S. O. Nam and M. Kuroki (2013) Tumor-targeted photodynamic therapy. *Anticancer Res.* **33**, 2823–2831.
11. Yousefpour, P. and A. Chilkoti (2014) Co-opting biology to deliver drugs. *Biotechnol. Bioeng.* **111**, 1699–1716.
12. Barok, M., H. Joensuu and J. Isola (2014) Trastuzumab emtansine: Mechanisms of action and drug resistance. *Breast Cancer Res.* **16**, 209.
13. Parker, N., M. J. Turk, E. Westrick, J. D. Lewis, P. S. Low and C. P. Leamon (2005) Folate receptor expression in carcinomas and normal tissues determined by a quantitative radioligand binding assay. *Anal. Biochem.* **338**, 284–293.
14. Leamon, C. P. (2008) Folate-targeted drug strategies for the treatment of cancer. *Curr. Opin. Investig. Drugs* **9**, 1277–1286.
15. Chen, C., J. Ke, X. E. Zhou, W. Yi, J. S. Brunzelle, J. Li, E. L. Yong, H. E. Xu and K. Melcher (2013) Structural basis for molecular recognition of folic acid by folate receptors. *Nature* **500**, 486–489.
16. Xu, S., B. Z. Olenyuk, C. T. Okamoto and S. F. Hamm-Alvarez (2013) Targeting receptor-mediated endocytotic pathways with nanoparticles: Rationale and advances. *Adv. Drug Deliv. Rev.* **65**, 121–138.
17. Gravier, J., R. Schneider, C. Frochot, T. Bastogne, F. Schmitt, J. Didelon, F. Guillemin and M. Barberi-Heyob (2008) Improvement of meta-tetra(hydroxyphenyl)chlorin-like photosensitizer selectivity with folate-based targeted delivery. synthesis and in vivo delivery studies. *J. Med. Chem.* **51**, 3867–3877.
18. You, H., H. E. Yoon, P. H. Jeong, H. Ko, J. H. Yoon and Y. C. Kim (2015) Pheophorbide-a conjugates with cancer-targeting moieties for targeted photodynamic cancer therapy. *Bioorg. Med. Chem.* **23**, 1453–1462.
19. Xia, W. and P. S. Low (2010) Folate-targeted therapies for cancer. *J. Med. Chem.* **53**, 6811–6824.
20. Maeda, H., H. Nakamura and J. Fang (2013) The EPR effect for macromolecular drug delivery to solid tumors: Improvement of tumor uptake, lowering of systemic toxicity, and distinct tumor imaging in vivo. *Adv. Drug Deliv. Rev.* **65**, 71–79.
21. Elsadek, B. and F. Kratz (2012) Impact of albumin on drug delivery–new applications on the horizon. *J. Control Release* **157**, 4–28.
22. Tiruppathi, C., W. Song, M. Bergenfeldt, P. Sass and A. B. Malik (1997) Gp60 activation mediates albumin transcytosis in endothelial cells by tyrosine kinase-dependent pathway. *J. Biol. Chem.* **272**, 25968–25975.
23. Yardley, D. A. (2013) nab-Paclitaxel mechanisms of action and delivery. *J. Control Release* **170**, 365–372.
24. Salditt, M., S. N. Braunstein, R. D. Camerini-Otero and R. M. Franklin (1972) Structure and synthesis of a lipid-containing bacteriophage. X. Improved techniques for the purification of bacteriophage PM2. *Virology* **48**, 259–262.
25. Boiteux, S., T. R. O'Connor, F. Lederer, A. Gouyette and J. Laval (1990) Homogeneous Escherichia coli FPG protein. A DNA glycosylase which excises imidazole ring-opened purines and nicks DNA at apurinic/apyrimidinic sites. *J. Biol. Chem.* **265**, 3916–3922.
26. Fischer, C., S. P. Rothenberg and M. da Costa (1978) Preparation of a stable folate-sepharose complex for affinity chromatography. *Anal. Biochem.* **85**, 15–19.

27. Epe, B. and J. Hegler (1994) Oxidative DNA damage: Endonuclease fingerprinting. *Methods Enzymol.* **234**, 122–131.
28. Epe, B., H. Henzl, W. Adam and C. R. Saha-Moller (1993) Endonuclease-sensitive DNA modifications induced by acetone and acetophenone as photosensitizers. *Nucleic Acids Res.* **21**, 863–869.
29. Srere, P., G. Kosicki and R. Lumry (1961) Isotope rate effects with D2O in several systems. *Biochim. Biophys. Acta* **50**, 184.
30. Butzbach, K. and B. Epe (2013) Photogenotoxicity of folic acid. *Free Radic. Biol. Med.* **65**, 821–827.
31. Krokan, H. E., R. Standal and G. Slupphaug (1997) DNA glycosylases in the base excision repair of DNA. *Biochem. J.* **325**(Pt 1), 1–16.
32. Epe, B. (2012) DNA damage spectra induced by photosensitization. *Photochem. Photobiol. Sci.* **11**, 98–106.
33. Gonzalez, M. M., M. Vignoni, M. Pellon-Maison, M. A. Ales-Gandolfo, M. R. Gonzalez-Baro, R. Erra-Balsells, B. Epe and F. M. Cabrerizo (2012) Photosensitization of DNA by beta-carbolines: Kinetic analysis and photoproduct characterization. *Org. Biomol. Chem.* **10**, 1807–1819.
34. Foote, C. S. (1991) Definition of type I and type II photosensitized oxidation. *Photochem. Photobiol.* **54**, 659.
35. Adarsh, N., R. R. Avirah and D. Ramaiah (2010) Tuning photosensitized singlet oxygen generation efficiency of novel aza-BODIPY dyes. *Org. Lett.* **12**, 5720–5723.
36. Kim, S., T. Y. Ohulchanskyy, H. E. Pudavar, R. K. Pandey and P. N. Prasad (2007) Organically modified silica nanoparticles co-encapsulating photosensitizing drug and aggregation-enhanced two-photon absorbing fluorescent dye aggregates for two-photon photodynamic therapy. *J. Am. Chem. Soc.* **129**, 2669–2675.
37. Brown, S. (2008) Photodynamic Therapy - Two photons are better than one. *Nat. Photonics* **2**, 394–395.
38. Gonzalez, M. M., J. Arnbjerg, M. P. Denofrio, R. Erra-Balsells, P. R. Ogilby and F. M. Cabrerizo (2009) One- and two-photon excitation of beta-carbolines in aqueous solution: pH-dependent spectroscopy, photochemistry, and photophysics. *J. Phys. Chem. A* **113**, 6648–6656.
39. Hrsak, D., L. Holmegaard, A. S. Poulsen, N. H. List, J. Kongsted, M. P. Denofrio, R. Erra-Balsells, F. M. Cabrerizo, O. Christiansen and P. R. Ogilby (2015) Experimental and computational study of solvent effects on one- and two-photon absorption spectra of chlorinated harmines. *Phys. Chem. Chem. Phys.* **17**, 12090–12099.
40. Hamblin, M. R. and E. L. Newman (1994) Photosensitizer targeting in photodynamic therapy. I. Conjugates of haematoporphyrin with albumin and transferrin. *J. Photochem. Photobiol., B* **26**, 45–56.
41. Alarcon, E., A. M. Edwards, A. M. Garcia, M. Munoz, A. Aspee, C. D. Borsarelli and E. A. Lissi (2009) Photophysics and photochemistry of zinc phthalocyanine/bovine serum albumin adducts. *Photochem. Photobiol. Sci.* **8**, 255–263.
42. Spring, B. Q., A. O. Abu-Yousif, A. Palanisami, I. Rizvi, X. Zheng, Z. Mai, S. Anbil, R. B. Sears, L. B. Mensah, R. Goldschmidt, S. S. Erdem, E. Oliva and T. Hasan (2014) Selective treatment and monitoring of disseminated cancer micrometastases in vivo using dual-function, activatable immunoconjugates. *Proc. Natl. Acad. Sci. U.S.A.* **111**, E933–E942.
43. Lee, R. J., S. Wang and P. S. Low (1996) Measurement of endosome pH following folate receptor-mediated endocytosis. *Biochim. Biophys. Acta* **1312**, 237–242.
44. Jeong, H., M. Huh, S. J. Lee, H. Koo, I. C. Kwon, S. Y. Jeong and K. Kim (2011) Photosensitizer-conjugated human serum albumin nanoparticles for effective photodynamic therapy. *Theranostics* **1**, 230–239.
45. Larroque, C., A. Pelegrin and J. E. Van Lier (1996) Serum albumin as a vehicle for zinc phthalocyanine: Photodynamic activities in solid tumour models. *Br. J. Cancer* **74**, 1886–1890.
46. Ol'shevskaya, V. A., R. G. Nikitina, A. N. Savchenko, M. V. Malshakova, A. M. Vinogradov, G. V. Golovina, D. V. Belykh, A. V. Kutchin, M. A. Kaplan, V. N. Kalinin, V. A. Kuzmin and A. A. Shtil (2009) Novel boronated chlorin e6-based photosensitizers: Synthesis, binding to albumin and antitumour efficacy. *Bioorg. Med. Chem.* **17**, 1297–1306.
47. Han, L., Y. Zhang, X. W. Chen, Y. Shu and J. H. Wang (2016) Protein-modified hollow copper sulfide nanoparticles carrying indocyanine green for photothermal and photodynamic therapy. *J. Mater. Chem. B* **4**, 105–112.
48. Du, C., D. Deng, L. Shan, S. Wan, J. Cao, J. Tian, S. Achilefu and Y. Gu (2013) A pH-sensitive doxorubicin prodrug based on folate-conjugated BSA for tumor-targeted drug delivery. *Biomaterials* **34**, 3087–3097.
49. Dosio, F., S. Arpicco, B. Stella, P. Brusa and L. Cattel (2009) Folate-mediated targeting of albumin conjugates of paclitaxel obtained through a heterogeneous phase system. *Int. J. Pharm.* **382**, 117–123.
50. Shen, Z., Y. Li, K. Kohama, B. Oneill and J. Bi (2011) Improved drug targeting of cancer cells by utilizing actively targetable folic acid-conjugated albumin nanospheres. *Pharmacol. Res.* **63**, 51–58.
51. Aits, S. and M. Jaattela (2013) Lysosomal cell death at a glance. *J. Cell Sci.* **126**, 1905–1912.
52. Tian, J., L. Ding, H. J. Xu, Z. Shen, H. Ju, L. Jia, L. Bao and J. S. Yu (2013) Cell-specific and pH-activatable rubyrin-loaded nanoparticles for highly selective near-infrared photodynamic therapy against cancer. *J. Am. Chem. Soc.* **135**, 18850–18858.
53. Vignoni, M., F. A. Rasse-Suriani, K. Butzbach, R. Erra-Balsells, B. Epe and F. M. Cabrerizo (2013) Mechanisms of DNA damage by photoexcited 9-methyl-beta-carbolines. *Org. Biomol. Chem.* **11**, 5300–5309.